Frequency Domain Modeling and Control of Fractional Order System for Permanent Magnet Synchronous Motor Velocity Servo System

Wei Yu[a,b], Ying Luo[b], YangQuan Chen[c], YouGuo Pi[b]

[a] *Department of Automation, Guang Dong University of Technology, Guangzhou, P.R. China. Email: yuweiscut@163.com*

[b] *Key Laboratory of Autonomous Systems and Network Control Ministry of Education,Department of Automation Science and Engineering, South China University of Technology, Guangzhou, P.R. China.*

[c] *Mechatronics, Embedded Systems and Automation (MESA) Lab, ME/EECS/SNRI/UCSolar, School of Engineering, University of California, Merced, 5200 N. Lake Road, Merced, CA 95343, USA*

Abstract

This paper presents fractional order system modeling and control for a permanent magnet synchronous motor (PMSM) velocity servo system. Fractional order model of the PMSM velocity servo system is obtained theoretically for an improved modeling precision. In order to identify the parameters of the proposed fractional order model, an enhancement of the classic Levy identification method with weights is applied. In a real-time PMSM velocity servo plant, the fractional order model is identified according to the experimental tests using the presented algorithm. The fact that the fractional model is more accurate than traditional integer order model is substantiated using by the mean square error performance index. Two H_∞ stabilizing output feedback controllers are designed for velocity servo using a simple scheme according to the identified fractional order model and the traditional integer order one, respectively. The experimental test performance using these two designed H_∞ controllers is compared to demonstrate the advantage of the proposed fractional order model of the PMSM velocity system.

Key words: Fractional order system; frequency modeling; system identification; permanent magnet synchronous motor

Preprint submitted to IET Control Theory and Applications *July 20, 2015*

1. INTRODUCTION

In recent years, studies of fractional calculus and its applications in various areas of sciences, engineering and industry have increased significantly, among which fractional order system control is an active area of research and development [1][2].The advantages of using fractional calculus in control applications are closed related to the the precision of modeling a system using fractional which has the memory and hereditary effects[3][4][5]. Thus the fractional calculus has been used for modeling in different application fields. Identification in the frequency domain is a particular case with great interest in applications[6]. For example, the memory effect in capacitor and inductor can be modeled by fractional derivative. Numerical experimental examples and measurements are shown to verify the fractional order characteristics of inductor[7][8].

Permanent magnet synchronous motors(PMSM) have been widely used in high precision motion control applications. The modeling and control of PMSM servo system can be found in many literatures[9][10]. Since the energy storage elements such as capacitor and inductor have the fractional order characteristics[11][12], the precise model of PMSM plant which includes the inductor should also be with fractional order characteristics. With the fractional order system identification method in time domain, a fractional order model of the PMSM velocity servo system is presented in [13]. It is known that fractional order operator is a kind of non-local operators with infinite dimensional characteristics[14]. Therefore, in the time domain, large amount of data needs to be collected for the fractional order dynamics as shown in [13].The frequency domain method is be used to identify fractional order system has two advantages, one is that it can avoid the difficulty of collect a large amount of data in the time domain. Moreover, a lot of mature theory and method in frequency domain identification for integer order system can be learned.

In this paper, a fractional order model is proposed for PMSM velocity control system, the effects of the two fractional orders in the model are discussed. A frequency domain system identification method is presented for the proposed fractional order system modeling. Frequencies responses data from real-time experimental tests are collected and the system identification method based on enhancing Levy identification algorithm with weights is presented. Two H_∞ stabilizing output feedback controllers for PMSM velocity servo are designed using a simple scheme according to the identified fractional order model and the traditional integer order one, respectively. The experimental velocity tracking performance using these two designed H_∞ stabilizing output feedback controllers is compared to demonstrate the advantage of the proposed fractional order model of the PMSM velocity system.

The major contributions of this paper include: (1) Fractional order model of the PMSM velocity servo system is obtained theoretically; (2) the fractional order model is identified according to the experimental tests using the system identification algorithm based on enhancing Levy identification method with weights; and (3) the fact that the fractional model is more accurate than traditional integer order model is demonstrated using the mean square error (MSE) performance index;

This paper is organized as follows: Sec. 2 presents the fractional order model for the PMSM velocity servo system. In Sec. 3, the new system identification scheme with weights enhancement based on the Levy identification method is discussed. The process of fractional order system identification is shown in Sec. 4. In Sec. 5, two H_∞ stabilizing output feedback controllers are designed with the same scheme according to the identified fractional order model and the traditional integer order one, and real-time experimental results are presented to demonstrate the advantage of the proposed fractional order model. The conclusion is given in Sec. 6.

2. Fractional Order Model for PMSM Velocity Servo System

According to the motor control theory, three-phase PMSM control can be similar to DC motor control by applying the space vector pulse width modulation (SVPWM) control strategy [15], as shown the equivalent circuit of synchronous motor in Fig.1 [16].

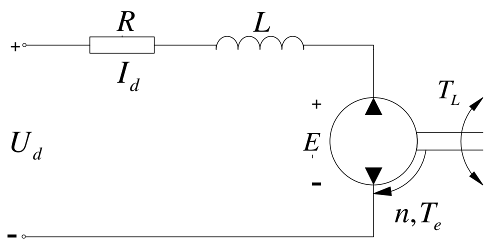

Figure 1: Equivalent circuit of synchronous motor.

Assuming the current of main circuit is continuous, the dynamic voltage equation is as following:

$$U_d = RI_d + L\frac{dI_d}{dt} + E \tag{1}$$

where U_d is the armature voltage, R is the stator resistance, I_d is the armature current, E is the back electromotive force (BEMF). Ignore the viscous friction and elastic torque, the dynamic equation of motor shaft is [17]

$$T_e - T_L = \frac{GD^2}{375}\frac{dn}{dt} \tag{2}$$

where T_e is electromagnetic torque, T_L is load torque of the motor , GD^2 is electric drive systems convert to the motor shaft of the flywheel moment of inertia [17]. Back electromotive force E and electromagnetic torque T_e can be expressed as:

$$E = C_e n \tag{3}$$

$$T_e = C_m I_d \tag{4}$$

where C_e is the electromotive force coefficient of motor, and C_m is the torque constant and $C_m = \frac{30}{\pi}C_e$, substituted into equation (1) and (2), we can get

$$U_d - E = R(I_d + T_l\frac{dI_d}{dt}) \tag{5}$$

$$I_d - I_{dL} = \frac{T_m}{R}\frac{dE}{dt} \tag{6}$$

where T_l is the electrical time constant and $T_l = \frac{L}{R}$, T_m is the mechanical time constant and $T_m = \frac{GD^2R}{375C_eC_m}$. I_{dL} is the external load current and $I_{dL} = \frac{T_L}{C_m}$. Under zero initial conditions, take the Laplace transformation on either side of the equation (5), the transfer function between the voltage and current is

$$\frac{I_d(s)}{U_d(s) - E(s)} = \frac{\frac{1}{R}}{T_l s + 1} \tag{7}$$

From equation (6), we can get the transfer function between the current and electromotive force as

$$\frac{E(s)}{I_d(s) - I_{dL}(s)} = \frac{R}{T_m s} \tag{8}$$

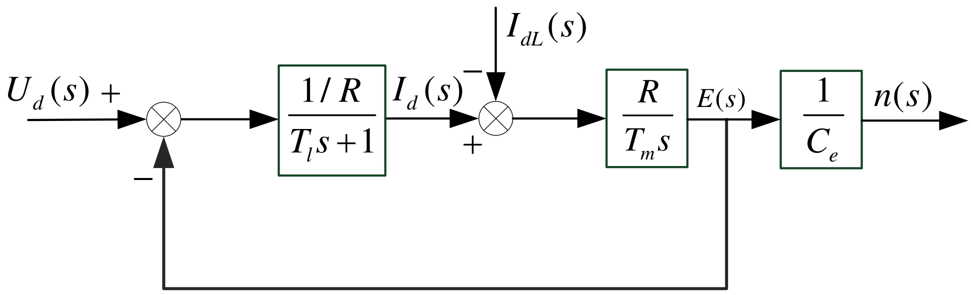

Figure 2: The dynamic block diagram of DC Motor.

Considering the velocity of motor $n = \frac{E}{C_e}$, the dynamic block diagram of direct current motor is shown in Fig. 2. The transfer function of PMSM velocity control system can be expressed as an integer model as follows:

$$G(s) = \frac{1/C_e}{T_m T_l s^2 + T_m s + 1} \tag{9}$$

In [11], a fractional model is identified to describe a three-dimensional network consisting of resistive and capacitive elements distributed across several interconnected layers. Meanwhile, considering the fact that the electrical characteristics of capacitor and inductor are fractional [8], the fractional order model of PMSM velocity control system is proposed as follows:

$$U_d - E = R(I_d + T_l \frac{dI_d^{\zeta}}{dt^{\zeta}}) \tag{10}$$

$$I_d - I_{dL} = \frac{T_m}{R} \frac{dE^{\vartheta}}{dt^{\vartheta}} \tag{11}$$

where ζ and ϑ are fractional orders. After the Laplace transform, the transfer function of PMSM velocity control can be expressed as

$$G(s) = \frac{1/C_e}{T_m T_l s^{\zeta+\vartheta} + T_m s^{\zeta} + 1}. \tag{12}$$

With fractional order ζ and ϑ changing from 1 to 0.1 in equation (12), the step response of integral and inertial element become faster, as shown in Fig. 3. In section 5 of experimental validation, this characteristic is validated on the experimental platform setup.

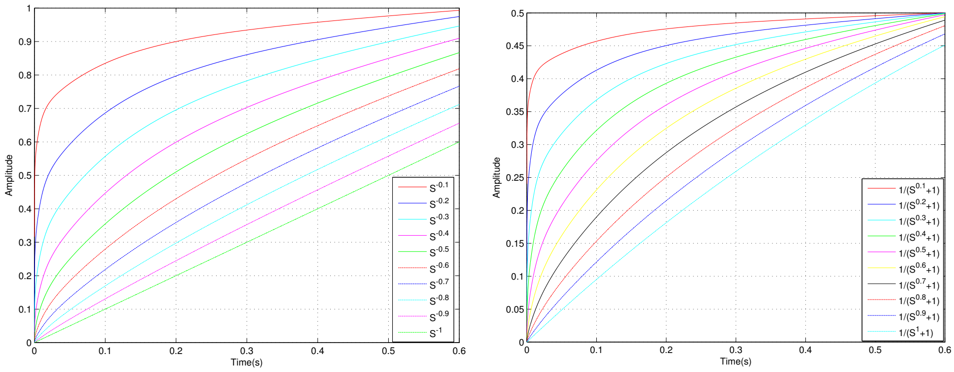

(a) Step response of integral element. (b) Step response of inertial element.

Figure 3: Step response of two elements for the PMSM fractional model.

Referring to the concept of continuous distribution order[18], the general fractional system can be transformed into commensurate order fractional system. Consequently, the equation (12) can be expressed as

$$G(s) = \frac{b_0}{a_2 s^{2q} + a_1 s^q + 1}. \tag{13}$$

Here, a_1, a_2, b_0, and q are the parameters to be identified. Applying this fractional order model (13), it is estimated that the characteristics of PMSM velocity control dynamics can be described more accurately over the traditional integer order model (9) since this fractional order feature in model (13) is closer to the nature of the components in PMSM [19][20].

3. System Identification of the Fractional Order Model

3.1. Fractional Order System Identification with Basic Levy's Method

According to the PMSM velocity servo system (13), the general transfer function of this fractional order model can be presented as,

$$\hat{G}(s) = \frac{b_0 + b_1 s^q + b_2 s^{2q} + \ldots + b_m s^{mq}}{a_0 + a_1 s^q + a_2 s^{2q} + \ldots + a_n s^{nq}} = \frac{\sum_{u=0}^{m} b_u s^{uq}}{\sum_{p=0}^{n} a_p s^{pq}}. \tag{14}$$

where m and n are zero or positive integers, and q is a positive fractional order number. Without loosing generality, we set $a_0 = 1$. The frequency response of (14) is

$$\hat{G}(j\omega) = \frac{\sum_{u=0}^{m} b_u (j\omega)^{uq}}{1 + \sum_{p=1}^{n} a_p (j\omega)^{pq}} = \frac{N(j\omega)}{D(j\omega)} = \frac{\alpha(\omega) + j\beta(\omega)}{\sigma(\omega) + j\tau(\omega)}. \tag{15}$$

α,β, are the real and imagine parts of numerator N respectively; σ,τ are the real and imagine parts of denominator D respectively; So, we have

$$\begin{cases} \alpha(\omega) = \sum_{u=0}^{m} b_u Re[(j\omega)^{uq}], \\ \sigma(\omega) = \sum_{p=0}^{n} a_p Re[(j\omega)^{pq}] = 1 + \sum_{p=1}^{n} a_p Re[(j\omega)^{pq}], \\ \beta(\omega) = \sum_{u=0}^{m} b_u Im[(j\omega)^{uq}], \\ \tau(\omega) = \sum_{p=1}^{n} a_p Im[(j\omega)^{pq}]. \end{cases} \tag{16}$$

The error between the identified model and the real plant, for a given frequency ω, will be

$$\epsilon(j\omega) = G(j\omega) - \frac{N(j\omega)}{D(j\omega)}. \tag{17}$$

Minimizing this error for an accurate system model identification would be an obvious but difficult way by adjusting the parameters in (14). Instead of this, Levy's method minimizes the square of the following norm [22]:

$$E(j\omega) \overset{\text{def}}{=} \epsilon(j\omega)D(j\omega) = G(j\omega)D(j\omega) - N(j\omega). \tag{18}$$

Omitting the frequency argument ω to simplify the notation, we have

$$\begin{aligned} E = GD - N &= [Re(G) + jIm(G)](\sigma + j\tau) - (\alpha + j\beta) \\ &= [Re(G)\sigma - Im(G)\tau - \alpha] + j[Re(G)\sigma + Im(G)\tau - \beta]. \end{aligned} \tag{19}$$

Since $|E|^2 = EE^*$, and $E^*(j\omega) = G^*(j\omega)D^*(j\omega) - N^*(j\omega)$, in order to get the minimal norm of E, we can get the following partial derivative equations with respect to one of the coefficients $a_p(p = 1, 2, ..., n)$ or $b_u(u = 0, 1, ..., m)$

$$\frac{\partial E}{\partial a_p} E^* + E \frac{\partial E^*}{\partial a_p} = 0 \qquad a_p = a_1, a_2, \ldots, a_n. \tag{20}$$

$$\frac{\partial E}{\partial b_u} E^* + E \frac{\partial E^*}{\partial b_u} = 0 \qquad b_u = b_0, b_1, \ldots, b_m. \tag{21}$$

From (15), it can be seen that

$$\frac{\partial E}{\partial a_p} = G(\omega)(j\omega)^{pq}, \qquad \frac{\partial E^*}{\partial a_p} = G^*(\omega)(-j\omega)^{pq}. \tag{22}$$

$$\frac{\partial E}{\partial b_u} = -(j\omega)^{uq}, \quad \frac{\partial E^*}{\partial b_u} = -(-j\omega)^{uq}. \tag{23}$$

Define $A(\omega) \overset{\text{def}}{=} |G(\omega)|$, $\varphi(\omega) \overset{\text{def}}{=} arg[G(\omega)]$, Then $G(\omega)$ and $G^*(\omega)$ can be expressed as following: $G(\omega) = A(\omega)e^{j\varphi(\omega)}$, $G^*(\omega) = A(\omega)e^{-j\varphi(\omega)}$, Omitting the frequency ω to simplify the notation, (20) and (21) lead to

$$\begin{cases} (G^*D^* - N^*)G(j\omega)^{pq} + (GD - N)G^*(-j\omega)^{pq} = 0 \\ -(G^*D^* - N^*)(j\omega)^{uq} - (GD - N)G^*(-j\omega)^{uq} = 0 \end{cases} \Rightarrow$$

$$\begin{cases} G^*G(D^*j^{pq} + D(-j)^{pq}) - N^*Gj^{pq} - NG^*(-j)^{pq} = 0 \\ G^*(D^*j^{uq} + GD(-j)^{uq}) - N^*j^{uq} - N(-j)^{uq} = 0 \end{cases} \Rightarrow$$

$$\begin{cases} A^2 \sum_{i=0}^{n} \{a_i[(-j)^{iq}j^{pq} + j^{iq}(-j)^{pq}]\omega^{iq}\} \\ -A \sum_{i=0}^{m} \{b_i[(-j)^{iq}j^{pq}e^{j\varphi} + j^{iq}(-j)^{pq}e^{-j\varphi}]\omega^{iq}\} = 0 \\ p = 1, \cdots, n \\ \quad A \sum_{i=0}^{n} \{a_i[e^{-j\varphi}(-j)^{iq}j^{uq} + e^{j\varphi}j^{iq}(-j)^{uq}]\omega^{iq}\} - \\ \quad \sum_{i=0}^{m} \{b_i[(-j)^{iq}j^{uq} + j^{iq}(-j)^{uq}]\omega^{iq}\} = 0 \\ \quad u = 0, \cdots, m \end{cases} \tag{24}$$

The results of Levy's method are not equally good at all frequencies [21], but this last step helps address the problem. With $\pm j = e^{\pm j(\pi/2)}$ and $e^{jx} = cosx + jsinx$, we can get $e^{jx} + e^{-jx} = 2cosx$. So,

$$(-j)^{iq}j^{pq} + j^{iq}(-j)^{pq} = 2\cos\left[\frac{\pi}{2}q(p-i)\right] \tag{25}$$

$$(-j)^{iq}j^{pq}e^{j\varphi} + j^{iq}(-j)^{pq}e^{-j\varphi} = 2\cos\left[q\frac{\pi}{2}(p-i) + \varphi\right] \tag{26}$$

$$e^{-j\varphi}(-j)^{iq}j^{uq} + e^{j\varphi}j^{iq}(-j)^{uq} = 2\cos\left[q\frac{\pi}{2}(i-u) + \varphi\right] \tag{27}$$

Inserting (25),(26) and (27) into (24), we have

$$\begin{cases} A \sum_{i=0}^{n} \left\{a_i \cos\left[q(p-i)\frac{\pi}{2}\right]\omega^{iq}\right\} - \sum_{i=0}^{m} \left\{b_i \cos\left[\varphi + q(p-i)\frac{\pi}{2}\right]\omega^{iq}\right\} = 0 \\ p = 1, \cdots, n \\ A \sum_{i=0}^{n} \left\{a_i \cos\left[\varphi + q(i-u)\frac{\pi}{2}\right]\omega^{iq}\right\} - \sum_{i=0}^{m} \left\{b_i \cos\left[q(u-i)\frac{\pi}{2}\right]\omega^{iq}\right\} = 0 \\ u = 0, \cdots, m \end{cases} \tag{28}$$

Theoretically, data from only one frequency suffice to modeling the plant. But in practice, due to the noise and other system uncertainties, one frequency behavior of the plant cannot be trusted as the real frequency behavior of the plant in the whole frequency domain. Therefore, in order to get an accurate system model, the data with f frequencies are used for the system identification as shown in following equations:

$$\begin{cases} \sum_{g=1}^{f}\left(A_g\sum_{i=0}^{n}\left\{a_i\cos\left[q(p-i)\frac{\pi}{2}\right]\omega_g^{iq}\right\}-\sum_{i=0}^{m}\left\{b_i\cos\left[\varphi_g+q(p-i)\frac{\pi}{2}\right]\omega_g^{iq}\right\}\right)=0\\ p=1,\cdots,n\\ \sum_{g=1}^{f}\left(A_g\sum_{i=0}^{n}\left\{a_i\cos\left[\varphi_g+q(i-u)\frac{\pi}{2}\right]\omega_g^{iq}\right\}-\sum_{i=0}^{m}\left\{b_i\cos\left[q(u-i)\frac{\pi}{2}\right]\omega_g^{iq}\right\}\right)=0\\ u=0,\cdots,m \end{cases} \tag{29}$$

3.2. Fractional Order System Identification with Weights Enhancement

The reason we use the weights enhancement is to counterbalance a known issue of Levy's method which leads to the identified model well fitting in high frequency range but poor fitting in low frequency range [23] [24].

Therefore, we apply the enhancement by weighting each frequency dependent weight $w(\omega_g)\overset{\text{def}}{=}w_g$. When the weights enhancement is used, system (28) for a frequency ω_g becomes

$$\begin{cases} A_g\sum_{i=0}^{n}\left\{a_i\cos\left[q(p-i)\frac{\pi}{2}\right]\omega_g^{iq}w_g\right\}-\sum_{i=0}^{m}\left\{b_i\cos\left[\varphi_g+q(p-i)\frac{\pi}{2}\right]\omega_g^{iq}w_g\right\}=0\\ p=1,\cdots,n\\ A_g\sum_{i=0}^{n}\left\{a_i\cos\left[\varphi_g+q(i-u)\frac{\pi}{2}\right]\omega_g^{iq}w_g\right\}-\sum_{i=0}^{m}\left\{b_i\cos\left[q(u-i)\frac{\pi}{2}\right]\omega_g^{iq}w_g\right\}=0\\ u=0,\cdots,m \end{cases} \tag{30}$$

From equation (29), we can obtain

$$\begin{cases} \sum_{g=1}^{f}\left(A_g\sum_{i=0}^{n}\left\{a_i\cos\left[q(p-i)\frac{\pi}{2}\right]\omega_g^{iq}w_g\right\}-\sum_{i=0}^{m}\left\{b_i\cos\left[\varphi_g+q(p-i)\frac{\pi}{2}\right]\omega_g^{iq}w_g\right\}\right)=0\\ p=1,\cdots,n\\ \sum_{g=1}^{f}\left(A_g\sum_{i=0}^{n}\left\{a_i\cos\left[\varphi_g+q(i-u)\frac{\pi}{2}\right]\omega_g^{iq}w_g\right\}-\sum_{i=0}^{m}\left\{b_i\cos\left[q(u-i)\frac{\pi}{2}\right]\omega_g^{iq}w_g\right\}\right)=0\\ u=0,\cdots,m \end{cases} \tag{31}$$

The way to find reasonable values for weights is [21]

$$w_g = \begin{cases} \frac{\omega_2-\omega_1}{2\omega_1^2} & if \quad g=1 \\ \frac{\omega_{g+1}-\omega_{g-1}}{2\omega_g^2} & if \quad 1<g<f \\ \frac{\omega_g-\omega_{g-1}}{2\omega_g^2} & if \quad g=f \end{cases} \tag{32}$$

J is the mean square error (MSE) performance index given by

$$J = \frac{1}{f}\sum_{i=1}^{f}\left[G(j\omega)-\hat{G}(j\omega)\right]^2 \tag{33}$$

4. Frequency Domain Identification for the Fractional Order Model

4.1. Introduction to the Experimental Platform for System Identification

In this paper, a PMSM velocity control experimental platform is applied for the system identification of the proposed fractional order model and the control performance verification. As shown in Fig. 4, the Space Vector Pulse Width Modulation (SVPWM) [25] control scheme is applied for the PMSM control with sine wave voltage input signal. This SVPWM control is a scheme using 3-phase power inverter. This 3-phase inverter consists of three groups of power insulated-gate bipolar transistor (IGBT) power transistors. The details of the SVPWM control with 3-phase inverter are introduced in [15]. The motor speed is measured by the optical encoder mounted on the PMSM. The parameters of the PMSM applied in this platform is shown in Table 1.

Table 1: Nominal Parameters of the PMSM

Rated power	0.5 (kw)
Rated speed	2000 (r/min)
Rated torque	2.4 (N.m/Arms)
Armature resistance	2.43 (ohm)
Mechanical time constant (T_m)	9.0 (ms)
Electrical time constant(T_l)	3.2 (ms)
Number of poles	8
Moment of inertia	0.00121 (kg.m^2)

The real-time PMSM velocity control experimental platform is also presented for the control performance experimental validation. As shown in the

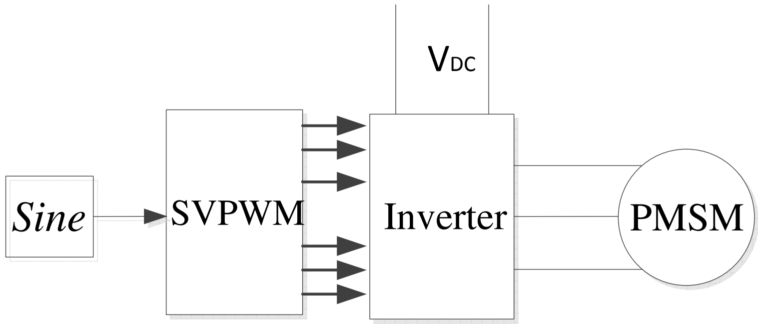

Figure 4: Block diagram of the experimental platform for system identification.

Fig. 5, the PMSM is controlled by the servo drive with JTAG emulator interface connecting to the computer for signal monitoring. The code composer studio software tool is used for the online tuning and debugging.

4.2. Frequency Domain Identification from Real-time Experiment

In fact, the essence of motor plant model is a low-pass filter, the definition of frequency domain range is depend on the applications. We choose 10 points in frequency range [0.1, 100], such as 0.1Hz, 0.5Hz, 1Hz, 2Hz, 5Hz, 10Hz, 20Hz, 50Hz, 80Hz, and 100Hz. The exact frequency responses of PMSM were recorded.

As shown in the Fig. 5, the code composer studio (CCS) software is used to record the input and output signals simultaneously. For example, fig. 6 shows speed response of the PMSM with input voltage sinusoidal waves, where the amplitude of voltage is 31V, and frequency equals to 10Hz. So we can get $A_6 = 20 * lg(48/31) = 3.79$, and $\varphi_6 = -79.74°$.

In order to decrease the influence of random errors, the experiment is repeated 10 times on each frequency and took the average. Table 2 are presented for frequencies in the following range $\omega \in [0.1, 100]$, to show the data for the system identification. Meanwhile, the results in Table 2 are illustrated in fig. 8 with stars.

Considering the fractional transfer function of PMSM velocity servo system (13) and the generalized form (14), it can be obtained $m = 0, n = 2$ in (14). Then the identification methods introduced in Section 3 can be applied. We choose f=10 and the definition range $q = (0, 1]$ with 0.01 interval, there-

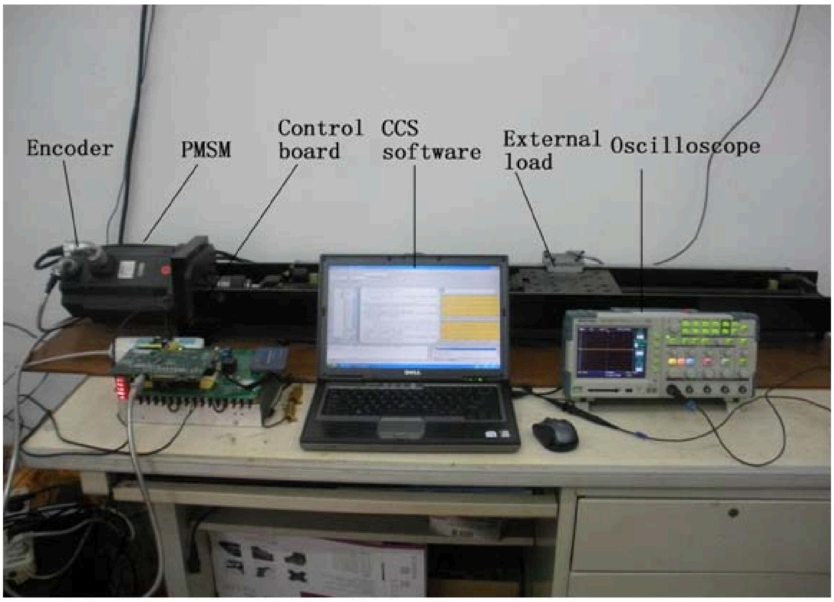

Figure 5: Experimental platform setup.

fore, $q = 0.01, 0.02, 0.03, \cdots 1$, according to equations (31) and (32), a_1, a_2, b_0 can be calculated from the following equations

$$\begin{cases} \sum_{g=1}^{10}\left(A_g \sum_{i=0}^{2}\left\{a_i \cos\left((1-i)\frac{q\pi}{2}\right)\omega_g^{iq} w_g\right\} - b_0 \cos\left[\varphi_g + \frac{q\pi}{2}\right] w_g\right) = 0 \\ \sum_{g=1}^{10}\left(A_g \sum_{i=0}^{2}\left\{a_i \cos\left((2-i)\frac{q\pi}{2}\right)\omega_g^{iq} w_g\right\} - b_0 \cos\left[\varphi_g + q\pi\right] w_g\right) = 0 \\ \sum_{g=1}^{10}\left(A_g \sum_{i=0}^{2}\left\{a_i \cos\left(\varphi_g + \frac{iq\pi}{2}\right)\omega_g^{iq} w_g\right\} - b_0 w_g\right) = 0 \end{cases} \quad (34)$$

Table 2: Data used in the system identification

Frequency (Hz)	0.1	0.5	1	2	5
Gain (dB)	15.85	15.45	14.73	12.84	8.72
Phase (deg)	-3.57	-13.81	-23.62	-38.47	-63.45
Frequency (Hz)	10	20	50	80	100
Gain (dB)	3.79	-1.86	-11.98	-17.53	-20.6
Phase (deg)	-79.74	-94.82	-119.47	-128.14	-135.41

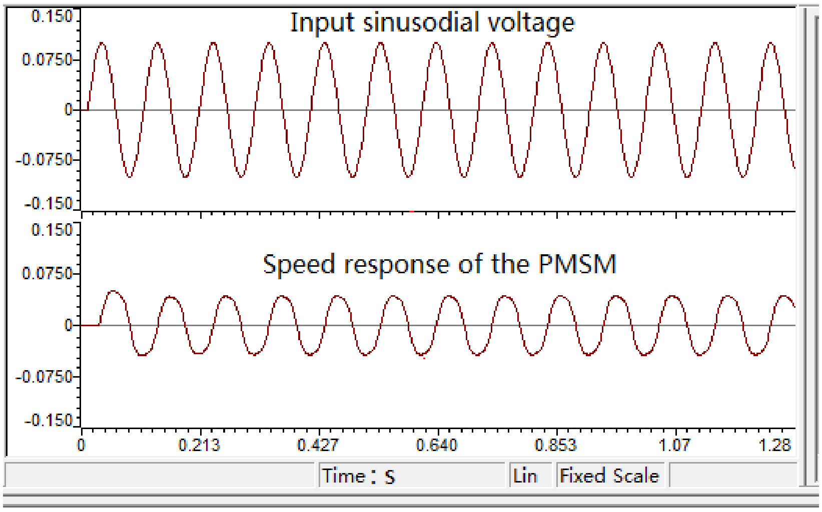

Figure 6: Speed response of the PMSM with sine wave voltage input.

According to the equation (32), the weights w_g equal to $w_1 = 20, w_2 = 1.8, w_3 = 2.25, w_4 = 0.18, w_5 = 0.225, w_6 = 0.01, w_7 = 0.0028, w_8 = 0.0031, w_9 = 0.0019, w_{10} = 0.0005$. We can obtain the MSE performance index J from equation (33) with the identified $\hat{G}(j\omega) = \hat{A}(\omega)e^{j\hat{\varphi}(\omega)}$ as following

$$J = \frac{1}{10}\sum_{g=1}^{10}\left[\Big(A(\omega)\cos(\varphi_g) - \hat{A}(\omega)\cos(\hat{\varphi}_g)\Big)^2 + \Big(A(\omega)\sin(\varphi_g) - \hat{A}(\omega)\sin(\hat{\varphi}_g)\Big)^2\right] \tag{35}$$

With $q = 0.01, 0.02, 0.03, \cdots 1$, Fig.7 shows the relationship between the MSE performance index J and fractional order q.

From fig.7, it can be seen that when q=0.87 with the parameters $a_1 = 0.097, a_2 = 0.00078$, and $b_0 = 6.28$, we can get the minimum of MSE performance index $J = 6.2 \times 10^{-4}$. Therefore, the fractional order model for the PMSM velocity servo system is identified as

$$G(s) = \frac{6.28}{0.00078s^{1.74} + 0.097s^{0.87} + 1}. \tag{36}$$

When q=1, from the equation (34), the parameters are calculated as $a_1 = 0.067, a_2 = 0.00015$, and $b_0 = 6.25$. the MSE performance index $J = 0.15$, the integer model of the PMSM velocity servo system is

$$G(s) = \frac{6.25}{0.00015s^2 + 0.067s + 1}. \tag{37}$$

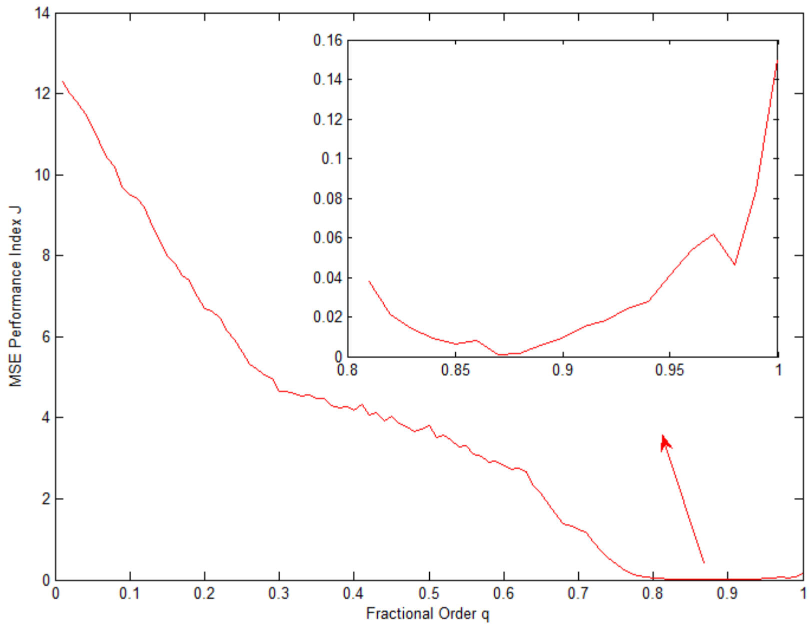

Figure 7: The relationship between q and J .

Figure 8 shows the Bode diagrams of the identified fractional order model (36) and integer order model (37). Obviously, the fractional order model (36) fits much better for the system identification frequency data marked as stars over the integer order model (37).

The results show the error of loop gain and fractional order are small between this fractional order model and the one in [13], as the internal structure of the machine is almost the same. Due to the nominal parameters of the PMSM are different, the coefficients of the denominator are not the same.

5. Experimental Validation

5.1. Experimental Setup

In order to verify that the identified fractional order model (36) of the PMSM velocity system is more precise than the traditional integer order one (37), the experimental validation is implemented with the block diagram as shown in Fig.9. Two H_∞ stabilizing output feedback controllers are designed for velocity servo system using the same simple scheme according to

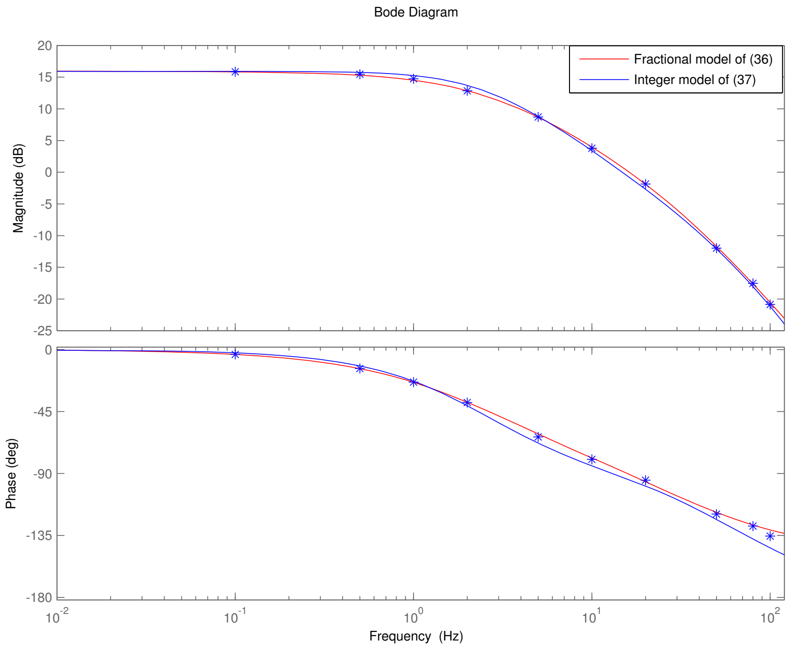

Figure 8: Bode diagrams of the identified models with the identification data in Table 2.

the identified fractional order model and the traditional integer order one, respectively.

$K(s)$ is the transfer matrix of a fractional order dynamic output feedback controller with pseudo-state space representation,

$$\begin{cases} D^v x_K(t) = A_K x_K(t) + B_K y(t) \\ u(t) = C_K x_K(t) + D_K y(t) \end{cases} \tag{38}$$

The pseudo-state space representation of G(s) is

$$\begin{cases} D^v x(t) = A_s x(t) + B_s u(t) \\ y(t) = C_s x(t) + D_s u(t) \end{cases} \tag{39}$$

The general control configuration for this H_∞ problem is derived by following theorem[26][27]: Fractional order system (39) of order v is BIBO stabilizable by output feedback control law (38) and $\left\|T^{cl}_{z\omega}\right\|_\infty < 1$ if there exist $Z = Z^T \in \mathbb{R}^{n\times n}$, $Y = Y^T \in \mathbb{R}^{n\times n}$, $\hat{A} \in \mathbb{R}^{n\times n}$, $\hat{B} \in \mathbb{R}^{n\times n_y}$, $\hat{C} \in \mathbb{R}^{n_u\times n}$,

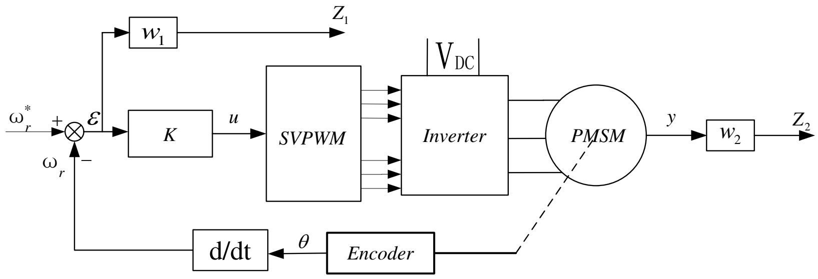

Figure 9: Block diagram of the experimental validation.

and $\hat{D} \in \mathbb{R}^{n_u \times n_y}$ such that LMI is feasible with

$$\begin{cases} D_K := \hat{D} \\ C_K := \left(\hat{C} - D_K C X\right) M^{-T} \\ B_K := N^{-1}\left(\hat{B} - Y B D_K\right) \\ A_K := N^{-1}\begin{pmatrix} \hat{A} - N B_K C X - Y B C_K M^T \\ -Y(A + B D_K \mathrm{C})X \end{pmatrix} M^{-T} \end{cases} \tag{40}$$

According to the fractional order model (36), with fractional order $v = 0.87$, we can get

$$A_s = \begin{pmatrix} 100 & -3.07 \\ 7723.85 & -224.36 \end{pmatrix}, B_s = \begin{pmatrix} 1 \\ -1 \end{pmatrix}, C_s = \begin{pmatrix} 1 & 1 \end{pmatrix}, D_s = 0 \tag{41}$$

Constraints $W_1(s)$ and $W_2(s)$ have respectively been added on the closed loop sensitivity function S(s) from w to ε , and on the complementary sensitivity function T(s) from w to y as shown in Fig.9. The closed-loop system sensitivity functions must verify

$$\|W_1 S\|_\infty < 1, \|W_2 T\|_\infty < 1 \tag{42}$$

This is equivalent to

$$\|S\|_\infty < \left\|W_1^{-1}\right\|_\infty, \|T\|_\infty < \left\|W_2^{-1}\right\|_\infty \tag{43}$$

Constraint W_1^{-1} static gain has been chosen low enough to cancel the closed-loop static error. Constraint W_2^{-1} has been chosen in order to attenuate

T(s) resonance and thus overshoot and oscillations in time response. Their transfer functions are

$$W_1^{-1}(s) = 3.15 \cdot \frac{s^{0.87} + 5.6 \times 10^{-4}}{s^{0.87} + 1} \tag{44}$$

$$W_2^{-1}(s) = 1.98 \times 10^{-5} \cdot \frac{s^{0.87} + 1.8 \times 10^{5}}{s^{0.87} + 1} \tag{45}$$

The output feedback controller is simply designed according to the (40), K such that $\left\| T_{z\omega}^{cl} \right\|_\infty < 1$, i.e.

$$\left\| \begin{array}{c} W_1 S \\ W_2 T \end{array} \right\|_\infty < 1 \tag{46}$$

Solver SDPT3 [28] is used to solve LMIs associated to theorem and thus to obtain controller K_1 given by relation (38) with

$$A_{K1} = \begin{pmatrix} -1.3 \times 10^5 & 3.2 \times 10^4 & 623.7 & -6.3 \times 10^6 \\ 1.3 \times 10^4 & -3.2 \times 10^3 & -62.3 & 6.3 \times 10^5 \\ -287.2 & 367.3 & -2.8 & 1.7 \times 10^4 \\ 0.82 \times 10^3 & -127.5 & 5.8 & -1.6 \times 10^5 \end{pmatrix}, D_{K1} = 1.8 \times 10^4$$
$$B_{K1} = \begin{pmatrix} -7.3 \times 10^6 \\ 7.3 \times 10^5 \\ 1.7 \times 10^5 \\ -1.8 \times 10^4 \end{pmatrix}, C_{K1} = \begin{pmatrix} 483.5 & -217 & -2.7 & 1.7 \times 10^5 \end{pmatrix}. \tag{47}$$

Relation (43) on the sensitivity functions is respected as shown in fig.10. According to the integer order model (37), with integer order $v = 1$, we can get

$$A_s = \begin{pmatrix} -262.6 & 1 \\ 41667 & -184 \end{pmatrix}, B_s = \begin{pmatrix} 1 \\ 0 \end{pmatrix}, C_s = \begin{pmatrix} 0 & 1 \end{pmatrix}, D_s = 0 \tag{48}$$

Solver SDPT3 [28] is used to solve LMIs associated to theorem and thus to

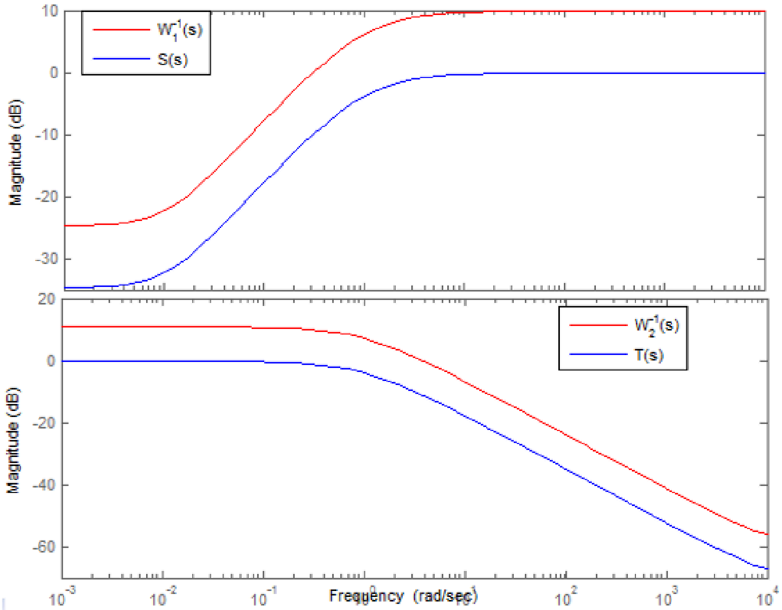

Figure 10: Constraints and sensitivity functions.

obtain controller K_2 given by relation (38) with

$$A_{K2} = \begin{pmatrix} -0.8\times10^5 & 2.1\times10^4 & 214.3 & -1.3\times10^6 \\ 0.8\times10^4 & -2.1\times10^3 & -21.4 & 1.3\times10^5 \\ -177.4 & 217.2 & -0.7 & 0.9\times10^4 \\ 0.41\times10^3 & -87.5 & 3.4 & -0.8\times10^5 \end{pmatrix}, D_{K2} = 0.9\times10^4$$

$$B_{K2} = \begin{pmatrix} -3.7\times10^6 \\ 3.7\times10^5 \\ 0.6\times10^5 \\ -0.7\times10^4 \end{pmatrix}, C_{K2} = \begin{pmatrix} 213.7 & -78 & -0.8 & 0.6\times10^5 \end{pmatrix}. \tag{49}$$

For the real-time experimental results, the speed responses with three reference speed inputs ω_r^*= 400rpm, 800rpm and 1200rpm, using the designed controllers K_1 and K_2 are presented in Fig.11, respectively. The red lines are the responses using K_1 controller based on the fractional order model, the blue lines are that using K_2 controller based on the integer order model. The main performance indicators are listed and compared in Table 3, where δ is the overshoot, and t_s is the settling time with steady-state error within 5%.

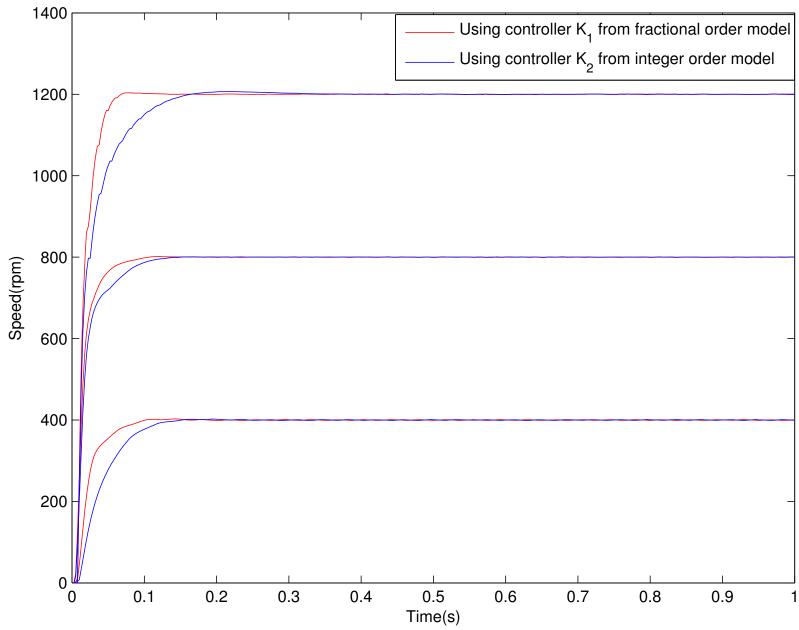

Figure 11: Speed responses comparison using K_1 and K_2 controllers.

Table 3: Tracking performance comparison

Velocity	δ with K_1	δ with K_2	t_s (s) with K_1	t_s (s) with K_2
400rpm	0	0	0.03	0.06
800rpm	0	0	0.04	0.07
1200rpm	0	1%	0.06	0.09

From the experimental comparison in Fig.11, it can be concluded that overall frequency range the real-time PMSM velocity servo system control with the identified fractional order model outperforms that with the identified traditional integer order model on velocity tracking performance.

6. Conclusion

In this paper, a fractional order model for a PMSM velocity servo system is suggested together with a system identification method. The fractional order model extends the traditional integer order model for the PMSM velocity servo system. The Levy system identification scheme in frequency domain is applied with an improvement scheme using weighting factors. This system identification scheme is applied for the system identification of the proposed fractional order model. Experimental data is used for demonstration that the fractional order model fits much better for the system identification frequency data over the integer order model. This may be explained by the nature of the distributed parameter system of the electromagnetism coupling thus may not be captured by integer finite order modeling while a fractional order modeling can offer potential to perform a better fitting. After the model parameters are estimated with real-time experimental results, two H_∞ stabilizing output feedback controllers are designed according to the identified fractional order and integer order models. The advantage of the proposed fractional order model over traditional integer order one is demonstrated by the fair experimental performance comparison.

References

[1] Gutierrez RE., Rosario JM.: 'Fractional Order Calculus: Basic Concepts and Engineering Applications', *Mathematical Problems in Engineering*, 2010, 1, pp. 1-19

[2] Kaczorek T.: 'Selected Topics in Theory of Fractional Systems'. *Bialystok, Poland: Tech. Univ. Bialystok*, 2009

[3] Torvik P.J., Bagley R.L.: 'On the appearance of the fractional derivative in the behavior of real material', *J of Applied Mechanics, transaction of the ASME*, 1984, 51, pp. 294-298

[4] Shen Jun., Lam James.: 'State-feedback H-infinity of commensurate fractional-order systems', *International Journal of Systems Science*, 2014, 45, (3), pp. 363-372

[5] Shen Jun., Lam James.: 'H-infinity model reduction for positive fractional order systems', *Asian Journal of Control*, 2014, 16, (2), pp. 441-450

[6] Gollee H., Mamma A., Loram ID.: 'Frequency-domain identification of the human controller', *Biological Cybernetics*, 2012, 106, (6-7), pp. 359-372

[7] Hartley T.T., Lorenzo C.F., Killory Qammer H.: 'Chaos in a fractional order Chua's system', *IEEE Transactions on Circuits and Systems*, 1995, 8, (42), pp. 485-490

[8] Petras I.: 'A note on the fractional-order Chua's system', *Chaos Solitons and Practals*, 2008, 38, pp. 140-147

[9] Prior G., Krstic M.: 'Quantized-Input Control Lyapunov Approach for Permanent Magnet Synchronous Motor Drives'. *IEEE Transactions on Control Systems Technology*, 2013, 21, (5), pp. 1784-1794

[10] Ortega R., Praly L., Astolfi A.: 'Estimation of Rotor Position and Speed of Permanent Magnet Synchronous Motors With Guaranteed Stability'. *IEEE Transactions on Control Systems Technology*, 2011, 19, (3), pp. 601-614

[11] Galvao RKH., Hadjiloucas S., Kienitz KH.: 'Fractional Order Modeling of Large Three-Dimensional RC Networks'. *IEEE Transactions on Circuits and Systems*, 2013, 60, (3), pp. 624-637

[12] Jesus I.S., Machado JAT.: 'Development of fractional order capacitors based on electrolyte processes'. *Nonlinear Dynamics*, 2009, 56, (1-2), pp. 45-55

[13] Wei Yu, Ying Luo, YuoGuo Pi.: 'Fractional order modeling and control for permanent magnet synchronous motor velocity servo system'. *Mechatronics*, 2013, 23, (7), pp. 813-820

[14] Ying Luo, YangQuan Chen.: 'Fractional Order Motion Controls'. *WILEY*, 2012

[15] Ying Luo, YangQuan Chen, YouGuo Pi.: 'Authentic Simulation Studies of Periodic Adaptive Learning Compensation of Cogging Effect in PMSM Position Servo System'. *Proceedings of the IEEE Chinese Conference on Decision and Control*, 2008, pp. 4760-4765

[16] Fitzgerald A.E.: 'Electric Machinery'. *House of Electronics Industry*, 2009

[17] BoShi Chen.: 'Electric power drag automatic control system-motion control system'. *China Machine Press*, 2003

[18] Hartley T.T., Lorenzo C.F.: 'Fractional-order system identification based on continuous order-distributions'. *Signal Process*, 2003, 83, (11), pp. 2287-2300

[19] Zilong Tang, Chaoxia, Simin Yu.: 'Design and Circuit Implementation of Fractional-Order Multiwing Chaotic Attractors'. *International Journal of Bifurcation and Chaos in Applied Sciences and Engineering*, 2012, 22, (11), pp. 1250269

[20] Yuan Gao, JianWen Fan, WenGuang Luo.: 'Chaos in the fractional order permanent magnet synchronous motor and its control'. *Journal of Wuhan University of Science and Technology*, 2012, 34, (7), pp. 134-140

[21] Vinagre B.: 'Modelado y Control de Sistemas Dinamicos Caracterizados por Ecuaciones Integro-Diferenciales de Orden Fractional'. *Ph.D. thesis*, 2001

[22] Levy E.: 'Complex Curve Fitting'. *IRE Transactions in Automatic Control*, 1959, 8, (1), pp. 37-44

[23] Valerio D., Ortigueira MD.: 'Identifying a Transfer Function From a Frequency Response'. *Journal of Computational and Nonlinear Dynamics*, 2008, 3, (2), pp. 71-77

[24] Dyer SA., Dyer JS.: 'Least-Squares Fitting of Data by Rational Functions: Levy's Method (Part 1)'. *IEEE Instrumentation and Measurement Magazine*, 2009, 12, (6), pp. 40-43

[25] Ying Luo, YangQuan Chen, YouGuo Pi.: 'Experimental study of fractional order proportional derivative controller synthesis for fractional order systems'. *Mechatronics*, 2011, 21, pp. 204-214

[26] Lamine Fadiga, Christophe Farges, Jocelyn Sabatier, Kevin Santugini.: ' H-infinity output feedback control of commensurate fractional order systems'. *12th European Control Conference (ECC)*, 2013, pp. 4538-4543

[27] Christophe Farges, Lamine Fadiga, Jocelyn Sabatier.: ' Hinfinity analysis and control of commensurate fractional order systems'. *M*echatronics, 2013, 23, (7), pp.772-780

[28] Toh K.C., Todd M.J., Tutuncu R.H.: 'SDPT3 - a matlab software package for semidefinite programming'. *Optimization Methods and Software*, 1998, 11, pp. 545-581